

Performance Evaluation of Approaches for Tracking Multiple Virus Particles in Fluorescence Microscopy Image Sequences

W. J. Godinez¹, M. Lampe², S. Wörz¹, B. Müller², R. Eils¹, and K. Rohr¹

¹University of Heidelberg, BIOQUANT, IPMB, and DKFZ Heidelberg,
Dept. Bioinformatics and Functional Genomics, Biomedical Computer Vision Group,
Im Neuenheimer Feld 267, 69120 Heidelberg, Germany

²University of Heidelberg, Dept. of Virology,
Im Neuenheimer Feld 324, 69120 Heidelberg, Germany

Abstract—Tracking virus particles in fluorescence microscopy image sequences enables the characterization of the dynamical behavior of these objects. Several approaches have been developed for the task of virus tracking. However, few studies have quantitatively evaluated the performance of the different approaches. Such a comparison is essential to predict the performance of the approaches under realistic conditions. In this paper, we present a quantitative evaluation of eight approaches for tracking virus particles. We have investigated deterministic and probabilistic approaches. The evaluation is based on nine real microscopy image sequences of virus particles, for which ground truth was obtained by manual tracking.

I. INTRODUCTION

Tracking single virus particles in fluorescence time-lapse microscopy images yields quantitative information that describes their dynamical behavior. Such information can be employed to characterize the influence of antiviral drugs. To obtain statistically sound conclusions, a large number of particles must be tracked. Therefore, automatic tracking approaches are required to efficiently handle the large amount of image data.

Several approaches for *virus tracking* have been described. Typically, *deterministic* approaches have been employed (e.g., [1], [2]). For work on other fluorescent biomolecular structures see, e.g., [3], [4], [5], [6], [7], [8]. More recently, *probabilistic* approaches for tracking virus particles (e.g., [9], [10]) have been introduced. For work on other fluorescent biomolecular structures see, e.g., [11], [12], [13]. However, quantitative comparisons of the performance of virus tracking approaches are rare. Such comparisons are needed to predict the performance of the approaches in real applications. The most extensive experimental comparisons of tracking approaches for fluorescent particles have been presented in [14], [15]. Both studies evaluate the performance of deterministic tracking approaches using synthetic images with different noise levels. The focus is on object localization and the evaluated approaches are based on four localization techniques: threshold-based localization, 2D Gaussian fitting, cross-correlation, and sum of absolute differences. One finding is that the performance of the tracking approaches declines as the signal-to-noise ratio (SNR) decreases. While the studies are relatively detailed, they have three shortcomings. First, the performance measure is based only on the localization error, and the influence of errors in

correspondence finding is ignored. Second, only deterministic approaches are considered. Third, no real images have been used.

In this work, we present a quantitative performance evaluation of approaches for tracking multiple virus particles in fluorescence microscopy image sequences. In total, we have evaluated eight tracking approaches. We have analyzed two deterministic approaches as well as six probabilistic approaches. The deterministic approaches are based on either the spot-enhancing filter [16] or 2D Gaussian fitting for particle localization, and a global nearest neighbor approach for motion correspondence. The probabilistic approaches are based on Kalman filters, a mixture of particle filters (MPF), and independent particle filters (IPF). The approaches have been applied to synthetic image sequences displaying virus-like objects, as well as to 9 different real microscopy image sequences (each comprising between 150 and 400 frames) displaying HIV-1 particles. In comparison to [14], [15], the employed performance measure reflects more comprehensively the performance of the evaluated tracking approaches. Additionally, deterministic as well as probabilistic approaches are evaluated. Finally, compared to [14], [15], we quantify the performance of the approaches based on real image sequences.

II. APPROACHES FOR TRACKING MULTIPLE VIRUS PARTICLES

Tracking comprises two main tasks: (1) *object representation and localization*, as well as (2) *motion correspondence and spatial-temporal filtering* [17]. Typically, deterministic approaches address only the tasks of object representation, localization, and motion correspondence. Probabilistic approaches include additionally a spatial-temporal filtering mechanism. In this section, we describe the investigated schemes for object representation, localization, motion correspondence, and spatial-temporal filtering. By combining the different schemes we obtain different tracking approaches. Finally, we introduce the employed performance measure.

A. Object Representation

For object representation we utilize a parametric approach. We describe the intensity distribution of a virus particle at time step t via a 2D Gaussian function, which is parametrized by

the location of the virus (x, y) , the peak intensity I_{max} , and the standard deviation σ_{xy} . The configuration of each virus particle is represented in a state vector $\mathbf{x}_t = (x, y, I_{max}, \sigma_{xy})$.

B. Object Localization

For object localization we investigate two approaches: an approach based on the spot-enhancing filter (SEF), and an approach using 2D Gaussian fitting (GaussFit). The first approach is a data-driven localization scheme consisting in applying a Laplacian-of-Gaussian (LoG) filter followed by a segmentation step via an intensity threshold that is dynamically adjusted over time. The second approach is a model-driven strategy where a 2D Gaussian function is fitted to candidate regions-of-interest (ROIs) determined by local intensity maxima. For each frame in an image sequence, each localization approach computes a set Z_t of *measured* position estimates. Each position estimate is defined as $\mathbf{z} = (x, y, I_{max}, \sigma_{xy})$.

C. Motion Correspondence

For motion correspondence, we use a global nearest neighbor (GNN) approach. Given a set X_t of N *predicted* position estimates and a set Z_t of N' *measured* position estimates, the aim of a motion correspondence algorithm is to find the associations between these two sets [18]. These associations can be encoded in a binary matrix \mathbf{A} , where the entries a_{ij} denote whether a match exists between a predicted position \mathbf{x}_t^i and a measured position \mathbf{z}_t^j . The global nearest neighbor scheme optimizes the matrix \mathbf{A} by minimizing the linear cost function Φ defined as the sum of the distances $d(\mathbf{x}_t^i, \mathbf{z}_t^j)$ induced by the set of correspondences encoded in \mathbf{A} . To optimize the matrix \mathbf{A} w.r.t. Φ , we employ the algorithm presented in [2], which is based on a graph-theoretical approach for the transportation problem.

D. Spatial-Temporal Filtering

Within the framework of sequential state estimation, the aim of a spatial-temporal filter is to estimate the state \mathbf{x}_t of a virus particle at time step t given a sequence of measurements $\mathbf{y}_{1:t}$. By representing the evolution of a virus via a *dynamical model* $p(\mathbf{x}_t|\mathbf{x}_{t-1})$, and incorporating measurements from the images via a *measurement model* $p(\mathbf{y}_t|\mathbf{x}_t)$, a Bayesian solution involves computing the *posterior* distribution $p(\mathbf{x}_t|\mathbf{y}_{1:t})$ using stochastic propagation and Bayes' theorem:

$$p(\mathbf{x}_t|\mathbf{y}_{1:t}) \propto p(\mathbf{y}_t|\mathbf{x}_t)p(\mathbf{x}_t|\mathbf{y}_{1:t-1}). \quad (1)$$

If the dynamical and measurement models are assumed to be linear and Gaussian, the recursion can be solved analytically using a Kalman filter. More generally, the recursive relation can be solved via approximation using a particle filter (e.g., [19]). The main idea behind this filter is to approximate the posterior distribution using a set of weighted random samples. For tracking multiple objects, one may track independently each object by using one Kalman filter per object (e.g., [20]). When tracking multiple objects with particle filters, multiple

modes arise in the posterior distribution computed over a one-body state space. The multimodality can be modeled via a non-parametric M -component mixture model, which can be computed using a mixture of particle filters [21] (see also [12] for an application to microtubuli growth). Analogous to the Kalman filter case, one may alternatively track multiple objects by instantiating one independent particle filter per object (e.g., [22]). To prevent the problem of *filter coalescence* that arises when employing independent particle filters, we here use an approach that includes a penalization scheme [10].

For both the Kalman filter as well as the particle filter, we adopt a random walk model to describe the temporal evolution of the state vector. For the Kalman filter, the measurement is defined as $\mathbf{y}_t = (x, y, I_{max}, \sigma_{xy})$ and thus the measurement model directly compares the predicted position estimate \mathbf{x}_t with the measured position estimate \mathbf{y}_t . For the particle filter, the measurement model quantifies the probability that a predicted sample generated a 2D Gaussian intensity distribution in an ROI \mathbf{y}_t centered at the predicted position (x, y) .

E. Evaluated Tracking Approaches

All approaches employ a 2D Gaussian intensity model to represent virus particles. The deterministic approaches are defined based on the different combinations of the localization schemes and the motion correspondence scheme. We have thus evaluated two deterministic approaches: 1) spot-enhancing filter with global nearest neighbor (SEF&GNN), and 2) 2D Gaussian fitting with global nearest neighbor (GaussFit&GNN). Note that the motion correspondence step requires a set X_t of predicted position estimates. For the deterministic schemes, a ‘‘predicted’’ position \mathbf{x}_t^i is given by the latest position estimate obtained for the tracked virus particle i at the previous time step $t - 1$.

The probabilistic approaches are analogously obtained by different combinations of the localization schemes and the spatial-temporal filters. We have thus investigated the following probabilistic approaches: 3) spot-enhancing filter and Kalman filters (SEF&Kalman), 4) spot-enhancing filter and a mixture of particle filters (SEF&MPF), 5) spot-enhancing filter and independent particle filters (SEF&IPF), 6) 2D Gaussian fitting and Kalman filters (GaussFit&Kalman), 7) 2D Gaussian fitting and a mixture of particle filters (GaussFit&MPF), and 8) 2D Gaussian fitting and independent particle filters (GaussFit&IPF). Note that the approaches using a mixture of particle filters can only track a fixed number of objects. The approaches using Kalman filters as well as those using independent particle filters require a motion correspondence step. For these approaches, we have employed the global nearest neighbor approach presented above.

F. Performance Measure

To quantitatively assess the performance of the approaches in each image sequence, we have employed the tracking accuracy

$$P_{track} = \frac{n_{track,correct}}{n_{track,total}}, \quad (2)$$

TABLE I: Description of real microscopy image sequences.

	Dimensions [pixels]	No. of time steps	No. of objects
Seq. 1	256×256	250	23
Seq. 2	256×256	250	10
Seq. 3	256×256	250	5
Seq. 4	256×256	150	21
Seq. 5	512×512	200	15
Seq. 6	512×512	400	29
Seq. 7	512×512	400	31
Seq. 8	512×512	400	43
Seq. 9	512×512	400	24

which reflects the ratio between the number of correctly computed trajectories $n_{track,correct}$ and the number of true trajectories $n_{track,total}$. The value $n_{track,correct}$ is computed as the weighted sum of the percentage of tracked time steps $r_{tracked,i}$ for each i -th true trajectory:

$$n_{track,correct} = \sum_{i=1}^{n_{track,total}} w_i r_{tracked,i}, \quad (3)$$

where the weight w_i is given by a Gaussian function $G(\cdot)$, which takes as its argument the number of correctly computed trajectories $n_{track,i}$ corresponding to each i -th true trajectory: $w_i = G(n_{track,i}; \mu = 1, \sigma = 1)$. The weighting scheme is introduced to penalize computed trajectories that are broken. A computed trajectory is assumed to be correct if the Euclidean distance between the measured object position and the true object position is below 2 pixels at each time step. Note that our performance measure integrates both localization errors and correspondence errors, and that $P_{track} \in [0, 1]$. Examples illustrating the measure P_{track} are shown in Fig. 1.

III. EXPERIMENTAL RESULTS

We have applied all eight tracking approaches to synthetic as well as real microscopy images. Below, we present the results for nine real microscopy image sequences each comprising between 150 and 400 frames. In these sequences, fluorescently labeled HIV-1 particles were imaged using a fluorescence wide-field microscope; movies were recorded with a frequency of 10Hz. Ground truth for the virus positions was obtained by manual tracking using the commercial software MetaMorph. For all sequences, we have employed fixed parameter values for all localization algorithms. Similarly, the noise parameters for the dynamical model of the Kalman filter were set analogously as the ones employed for the particle filter. Details for each sequence are given in Table I. The quantitative experimental results for the nine sequences are presented in Table II.

As an example, results for the real image sequence ‘‘Seq. 7’’ are shown in Fig. 2. It can be seen that the trajectories computed by the deterministic approach SEF&GNN exhibit large displacements, which are artefacts generated by wrong assignments. By introducing a spatial-temporal filtering step, such errors are reduced, as can be seen in the results of the probabilistic approach SEF&Kalman. The results for SEF&MPF are relatively good. However, only a fixed number of objects is tracked, which diminishes the performance. In

contrast, SEF&IPF handles a variable number of objects, thereby tracking more objects and achieving improved results.

These observations are further supported by the quantitative results in Table 2. The results indicate that the performance of the evaluated deterministic approaches is not very good (e.g., for the best deterministic approach, namely SEF&GNN, we obtain a mean tracking accuracy of $\bar{P}_{track} = 67.33\%$). One reason for this result is that localization errors (e.g., detection failures) as well as errors in correspondence finding (e.g. incorrect assignments) reduce the number of correctly computed trajectories. The approaches based on the Kalman filter yield an improved result in comparison to the deterministic approaches (e.g., $\bar{P}_{track} = 72.93\%$ for the best Kalman-based approach, namely SEF&Kalman). This suggests that the inclusion of a spatial-temporal filtering step enhances the performance. However, for the approaches using Kalman filters, object localization and spatial-temporal filtering are uncoupled. This implies that temporal information is not used for object localization, and likewise, image information is not directly used by the spatial-temporal filter. The approaches using MPF attain a relatively low tracking accuracy (e.g., $\bar{P}_{track} = 59.29\%$ for the best MPF-approach, namely SEF&MPF). One main reason for this result is that, in comparison to all other approaches, MPF cannot track a variable number of objects (whereas in the investigated images, the number of objects varies over time). Another reason is that MPF uses a variable number of samples to estimate each mixture component (usually corresponding to one object). As such, the estimation accuracy decreases for those components for which few samples have been assigned. In comparison, approaches using IPF yield very good results. In fact, the best result among all approaches is obtained by GaussFit&IPF with $\bar{P}_{track} = 78.74\%$. In contrast to MPF, IPF can handle a variable number of objects, and employs a constant number of samples for each tracked object. In contrast to approaches using the Kalman filter, IPF capitalizes on the effective use of spatial-temporal information by the particle filter, which integrates object localization, motion correspondence, and position estimation. We conducted a one-way ANOVA test and it turned out that the differences in performance between the different approaches are significant at $p < 0.05$.

IV. DISCUSSION

We have presented a performance evaluation of eight different approaches for tracking multiple virus particles in fluorescence microscopy images. We have evaluated deterministic as well as probabilistic approaches and quantified their performance for nine real microscopy image sequences. Our experimental results suggest that there are significant differences between the evaluated approaches in terms of the obtained tracking accuracy. It also turned out that the probabilistic approaches yield a better performance than the deterministic approaches.

REFERENCES

- [1] G. Seisenberger, M. U. Ried, T. Endress, H. Buning, M. Hallek, and C. Bräuchle, ‘‘Real-time single-molecule imaging of the infection pathway of an adeno-associated virus,’’ *Science*, vol. 294, no. 5548, pp. 1929–1932, 2001.

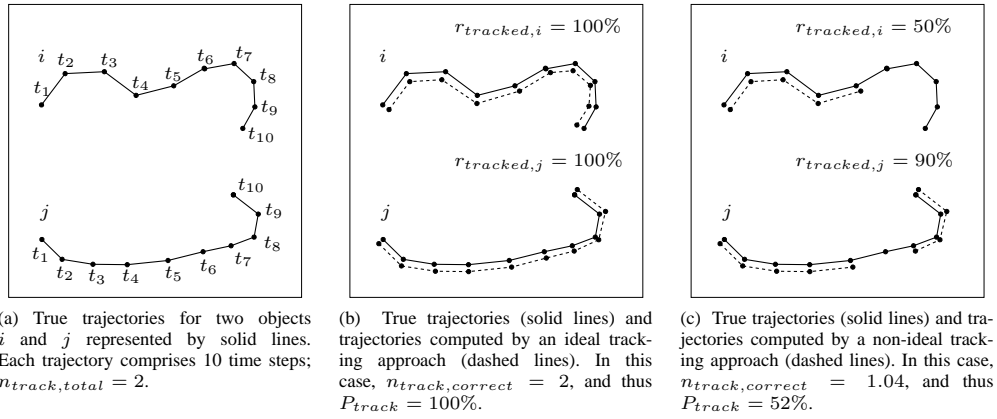


Fig. 1: Examples illustrating the performance measure P_{track} .

TABLE II: Tracking accuracy P_{track} for real microscopy image sequences.

	SEF& GNN	SEF& Kalman	SEF& MPF	SEF& IPF	GaussFit& GNN	GaussFit& Kalman	GaussFit& MPF	GaussFit& IPF
Seq. 1	75.24	81.12	84.82	86.73	71.29	81.30	81.95	82.61
Seq. 2	60.78	68.70	71.93	83.52	30.79	44.64	63.49	84.67
Seq. 3	45.07	32.29	76.67	42.55	40.69	60.18	60.00	80.00
Seq. 4	61.71	68.89	28.52	71.10	70.53	74.59	23.81	83.39
Seq. 5	93.54	93.54	84.64	93.54	81.09	93.54	85.64	93.54
Seq. 6	57.79	74.59	39.64	63.98	55.18	67.97	41.73	62.10
Seq. 7	64.65	80.60	48.26	82.48	53.21	77.47	31.23	77.67
Seq. 8	74.61	74.09	50.62	74.64	75.10	74.11	49.04	67.76
Seq. 9	72.55	82.55	48.51	73.55	67.78	80.55	52.61	76.89
Mean	67.33	72.93	59.29	74.68	60.63	72.71	54.39	78.74
Std. Dev.	13.68	17.08	20.62	15.00	16.82	13.99	20.96	9.32

- [2] I. F. Sbalzarini and P. Koumoutsakos, "Feature point tracking and trajectory analysis for video imaging in cell biology," *J. Struct. Biol.*, vol. 151, no. 2, pp. 182–195, 2005.
- [3] W. Tvarusko, M. Bentele, T. Misteli, R. Rudolf, C. Kaether, D. L. Spector, H. H. Gerdes, and R. Eils, "Time-resolved analysis and visualization of dynamic processes in living cells," *Proc. Natl. Acad. Sci. U.S.A.*, vol. 96, no. 14, pp. 7950–7955, 1999.
- [4] D. Thomann, D. R. Rines, P. K. Sorger, and G. Danuser, "Automatic fluorescent tag detection in 3D with super-resolution: application to the analysis of chromosome movement," *J. Microsc.*, vol. 208, pp. 49–64, Oct. 2002.
- [5] G. Yang, A. Matov, and G. Danuser, "Reliable tracking of large scale dense antiparallel particle motion for fluorescence live cell imaging," in *Proc. CVPR'05, Workshop on Computer Vision Methods for Bioinformatics*, San Diego, CA, USA, 2005, pp. 138–147.
- [6] V. Racine, A. Hertzog, J. Jouanneau, J. Salamero, C. Kervrann, and J.-B. Sibarita, "Multiple-target tracking of 3d fluorescent objects based on simulated annealing," in *Proc. ISBI'06*, Arlington, VA, USA, 2006, pp. 1020–1023.
- [7] K. Jaqaman, D. Loerke, M. Mettlen, H. Kuwata, S. Grinstein, S. L. Schmid, and G. Danuser, "Robust single-particle tracking in live-cell time-lapse sequences," *Nat. Meth.*, vol. 5, no. 8, pp. 695–702, 2008.
- [8] L. Cortes and Y. Amit, "Efficient annotation of vesicle dynamics in video microscopy," *IEEE Trans. Pattern Anal. Mach. Intell.*, vol. 30, no. 11, pp. 1998–2010, 2008.
- [9] N. Arhel, A. Genovesio, K. Kim, S. Miko, E. Perret, J.-C. Olivo-Marin, S. Shorte, and P. Charneau, "Quantitative four-dimensional tracking of cytoplasmic and nuclear HIV-1 complexes," *Nat. Methods*, vol. 3, no. 10, pp. 817–824, 2006.
- [10] W. J. Godinez, M. Lampe, S. Wörz, B. Müller, R. Eils, and K. Rohr, "Probabilistic tracking of virus particles in fluorescence microscopy images," in *Proc. ISBI'08*, Paris, France, May 2008, pp. 272–275.
- [11] N. Chenouard, I. Bloch, and J.-C. Olivo-Marin, "Feature-aided particle tracking," in *Proc. ICIP'08*, San Diego, CA, USA, Oct 2008, pp. 1796–1799.
- [12] I. Smal, K. Draegestein, N. Galjart, W. Niessen, and E. Meijering, "Particle filtering for multiple object tracking in dynamic fluorescence microscopy images: Application to microtubule growth analysis," *IEEE Trans. Med. Imaging*, vol. 27, no. 6, pp. 789–804, June 2008.
- [13] J. W. Yoon, A. Bruckbauer, W. J. Fitzgerald, and D. Klenerman, "Bayesian inference for improved single molecule fluorescence tracking," *Biophys. J.*, vol. 94, no. 12, pp. 4932–4947, 2008.
- [14] M. K. Cheezum, W. F. Walker, and W. H. Guilford, "Quantitative comparison of algorithms for tracking single fluorescent particles," *Biophys. J.*, vol. 81, no. 4, pp. 2378–2388, 2001.
- [15] B. C. Carter, G. T. Shubeita, and S. P. Gross, "Tracking single particles: a user-friendly quantitative evaluation," *Phys. Biol.*, vol. 2, no. 1, pp. 60–72, 2005.
- [16] D. Sage, F. R. Neumann, F. Hediger, S. M. Gasser, and M. Unser, "Automatic tracking of individual fluorescence particles: Application to the study of chromosome dynamics," *IEEE Trans. Image Process.*, vol. 14, no. 9, pp. 1372–1382, 2005.
- [17] D. Comaniciu, V. Ramesh, and P. Meer, "Kernel-based object tracking," *IEEE Trans. Pattern. Anal. Mach. Intell.*, vol. 25, no. 5, pp. 564–575, 2003.
- [18] I. J. Cox, "A review of statistical data association for motion correspondence," *Int. J. Comput. Vision*, vol. 10, no. 1, pp. 53–66, 1993.
- [19] M. Isard and A. Blake, "CONDENSATION – conditional density propagation for visual tracking," *Int. J. Comput. Vision*, vol. 29, no. 1, pp. 5–28, 1998.
- [20] C. Rasmussen and G. D. Hager, "Probabilistic data association methods for tracking complex visual objects," *IEEE Trans. Pattern. Anal. Mach. Intell.*, vol. 23, no. 6, pp. 560–576, 2001.
- [21] J. Vermaak, A. Doucet, and P. Pérez, "Maintaining multi-modality through mixture tracking," in *Proc. ICCV'03*, Nice, France, October 2003, IEEE, pp. 1110–1116.
- [22] W. Qu, D. Schonfeld, and M. Mohamed, "Real-time interactively distributed multi-object tracking using a magnetic-inertia potential model," in *Proc. ICCV'05*, Beijing, China, October 2005, IEEE, pp. 535–540.

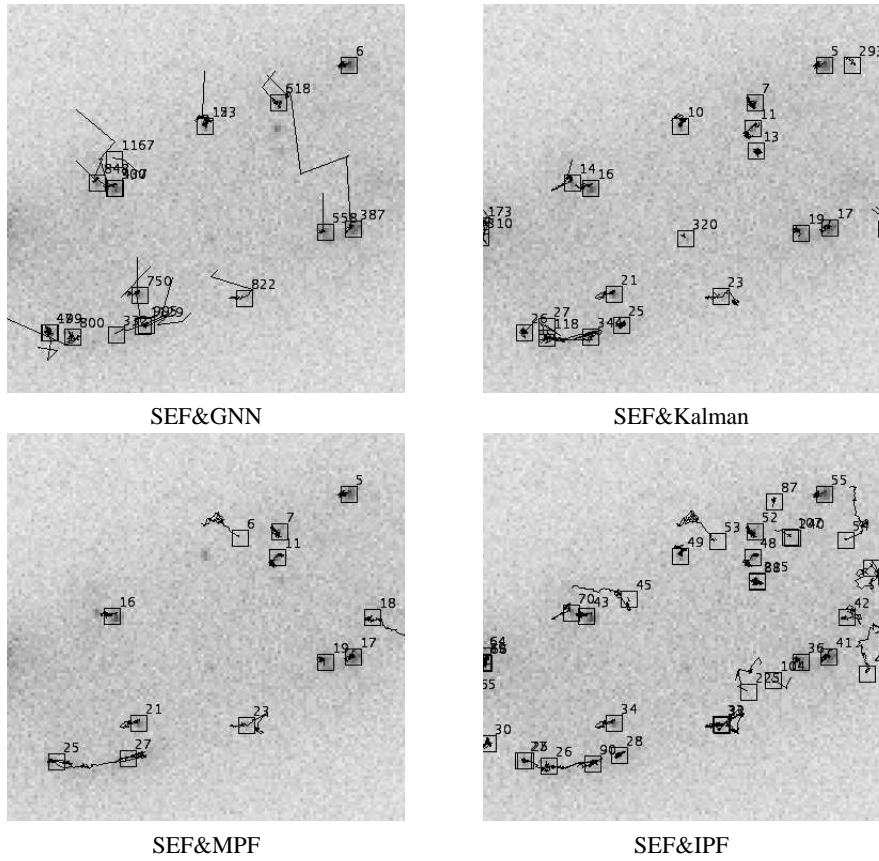


Fig. 2: Tracking results of four approaches for the real image sequence “Seq. 7” (time step $t = 110$).